Gaze and the Control of Foot Placement When Walking in Natural Terrain

Highlights

- Gaze and full-body kinematics were recorded during real-world locomotion

- Walkers show distinct gaze strategies appropriate for the demands of each terrain

- Nevertheless, walkers also adopted a constant look-ahead time across all terrains

- Walkers tune gaze behavior to sustain consistent locomotor strategy in all terrains

Authors

Jonathan Samir Matthis,
Jacob L. Yates, Mary M. Hayhoe

Correspondence

matthis@utexas.edu

In Brief

Matthis et al. recorded subjects' gaze and full-body kinematics during real-world locomotion. Walkers show distinct gaze strategies appropriate for the demands of each terrain. Nevertheless, walkers also adopted a constant look-ahead time across all terrains. Walkers tune gaze behavior to sustain consistent locomotor strategy in all terrains.

Gaze and the Control of Foot Placement When Walking in Natural Terrain

Jonathan Samir Matthis,[1,4,*] Jacob L. Yates,[2,3] and Mary M. Hayhoe[1]
[1]Center for Perceptual Systems, University of Texas at Austin, Austin, TX, USA
[2]Center for Visual Science, University of Rochester, Rochester, NY, USA
[3]Brain and Cognitive Science, University of Rochester, Rochester, NY, USA
[4]Lead Contact
*Correspondence: matthis@utexas.edu
https://doi.org/10.1016/j.cub.2018.03.008

SUMMARY

Human locomotion through natural environments requires precise coordination between the biomechanics of the bipedal gait cycle and the eye movements that gather the information needed to guide foot placement. However, little is known about how the visual and locomotor systems work together to support movement through the world. We developed a system to simultaneously record gaze and full-body kinematics during locomotion over different outdoor terrains. We found that not only do walkers tune their gaze behavior to the specific information needed to traverse paths of varying complexity but that they do so while maintaining a constant temporal look-ahead window across all terrains. This strategy allows walkers to use gaze to tailor their energetically optimal preferred gait cycle to the upcoming path in order to balance between the drive to move efficiently and the need to place the feet in stable locations. Eye movements and locomotion are intimately linked in a way that reflects the integration of energetic costs, environmental uncertainty, and momentary informational demands of the locomotor task. Thus, the relationship between gaze and gait reveals the structure of the sensorimotor decisions that support successful performance in the face of the varying demands of the natural world.

INTRODUCTION

The human evolutionary lineage diverged from the apes with the adaptation toward striding bipedalism [1]. Bipedal locomotion affords many distinct adaptive advantages: it frees the forelimbs from locomotor responsibilities, increases the field of view, and is exceptionally energetically efficient [2–4]. However, our unique form of locomotion also confers a major disadvantage—striding bipedalism is inherently unstable. A bipedal walker must commit the full momentum of their body to every step, so each selected foothold must support the walker's bodyweight while also facilitating the transition to the subsequent step. Consequently, human locomotion over irregular terrain relies as much on the ability

to efficiently gather information about the upcoming path as it does on the physical dynamics of the bipedal gait cycle.

When walking through flat, obstacle-free environments, vision is not needed to guide foot placement. In simple terrains where footholds are unconstrained, humans exhibit a robust drive to select a preferred gait cycle comprising an optimal combination of step length, width, and duration that minimizes the energetic cost of transport by exploiting the passive physical dynamics of bipedal gait [5–8]. Existing models of locomotion focus primarily on the optimization of the preferred gait cycle against internal neural and biomechanical factors [9, 10]. However, locomotion over rough terrain must be optimized for both the internal structure of the walker and the external structure of the environment being traversed. In these environments, a walker must make a trade-off between the efficiency of the preferred gait cycle and the need to place the feet in viable locations to support continuous locomotion. Little is known about how vision is used to identify viable footholds and how walkers use this information to alter the preferred gait cycle appropriately for the upcoming path. Previous studies tracking the eyes while walking outdoors have found alterations of gaze with the demands of the terrain [11–14], but foot placement was not measured, so it is not possible to analyze the precise relation between gaze and foot placement. Additionally, in these studies, the terrain placed only moderate demands on stability.

Studies investigating the relationship between gaze and stepping in the laboratory have demonstrated that walkers tend to fixate the ground around two steps ahead [15–20]. In experiments that manipulated the available visual stimulus, Matthis and Fajen [21, 22] showed that planning two steps ahead may help humans approximate the energetic savings of the preferred gait cycle during locomotion over complex terrain by minimizing the need for active muscular intervention when avoiding obstacles on a path. This strategy allows the walker to initialize the mechanical state of their body before the beginning of each step so that the resulting trajectory of the center of mass (COM) will facilitate stepping on the targeted footholds [23]. By utilizing information about upcoming footholds during a critical phase of the gait cycle between midstance and toe off of the preceding step, walkers are able to step accurately on their desired location while efficiently exploiting the physical dynamics of bipedal gait [24, 25].

Although these findings are suggestive of the nature of the visual control of foot placement, it remains an open question how the information necessary to enact this strategy is acquired
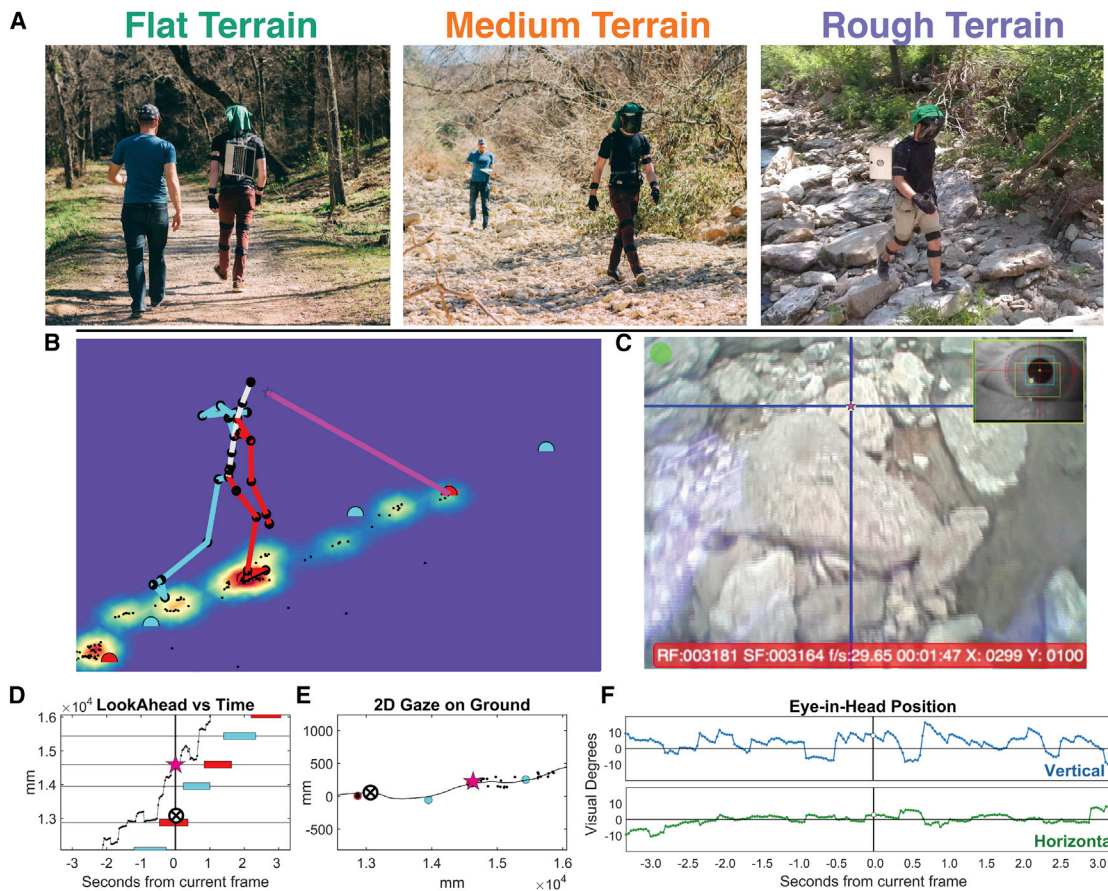
Figure 1. Terrain Types and Data Reconstruction

(A) Subjects walked over three different types of natural terrain: Flat, Medium, and Rough.

(B–E) A sample frame from Video S1, which depicts the full-body kinematic and 3D gaze data used in this study. (B) The reconstructed skeleton and 3D gaze vector (pink line) of a subject walking in the Rough terrain condition. The red and cyan dots show upcoming footholds. Intersections between the subject's 3D gaze and the groundplane are shown as small black dots, and the Gaussian heatmap represents the kernel density estimate of these gaze-groundplane intersection points—that is, regions where the walker has fixated appear as hotspots. (C) A frame from the Positive Science eye tracker, with the subject's 2D point of regard shown as the blue crosshairs. These data were used to calculate subject's 3D gaze (pink line in [B]; see STAR Methods). (D) A plot of subjects' look-ahead versus time. The black trace represents subjects gaze on the ground along the primary direction of locomotor versus time. The crossed circle shows the position of the subjects' center of mass (COM), and the pink star shows their current gaze-on-ground position, so the vertical distance between the COM and the star represents the subject's current look-ahead distance. Horizontal red and cyan bars show the location and duration of upcoming right and left footholds, respectively. In the frame depicted here, the subject is supported over on their right foot (red horizontal bar) while looking ahead near the location of their next upcoming right foothold. (E) A 2D top-down view of subject's gaze and footholds. Crossed circle and black line show the subject's COM position and trajectory, and the pink star shows the subject's current gaze-on-ground position. Black dots show upcoming gaze data, and red and cyan dots show upcoming right and left footholds. This subplot is essentially a simplified, top-down view of the groundplane represented in (B).

(F) Traces of the subject's eye-in-head position in the vertical (blue line, top) and horizontal (green line, bottom) dimensions. Each dot corresponds to one frame of eye-tracking data (30 fps [frames per second]). Note that fixations on the ground during locomotion require the subject to move their eyes downward at a constant velocity, resulting in the sawtooth-like pattern of the gaze trace in the vertical axis (as opposed to the square-wave-like shape of fixations when stationary). Combining these slow, downward eye movements with the movements of the head and body during locomotion results in the stable fixations on the ground shown in (D) and Video S1. An external video of a subject walking in the Rough terrain condition is presented in Video S2.

during locomotion in a natural environment. In the studies discussed above, obstacles and footholds were patches of light on flat ground, and the visibility and location of the patches were artificially manipulated. How do walkers acquire the visual information needed to guide foot placement in natural environments? How does the drive to move efficiently interact with the need to place the foot in stable locations? To answer these questions during natural walking, we developed a system that integrates 3D gaze and full-body motion capture of subjects walking

in unconstrained outdoor environments. We found that not only do walkers adapt their gaze behavior to the specific information needed to traverse terrains of varying complexity but that they do so in a way that maintains a constant temporal look-ahead window across all terrains. It appears that walkers tune the coupling between gaze and foot placement to the uncertainty of the upcoming path in order to maintain a consistent locomotor strategy that balances the need to move efficiently with the need to place the feet on stable locations.
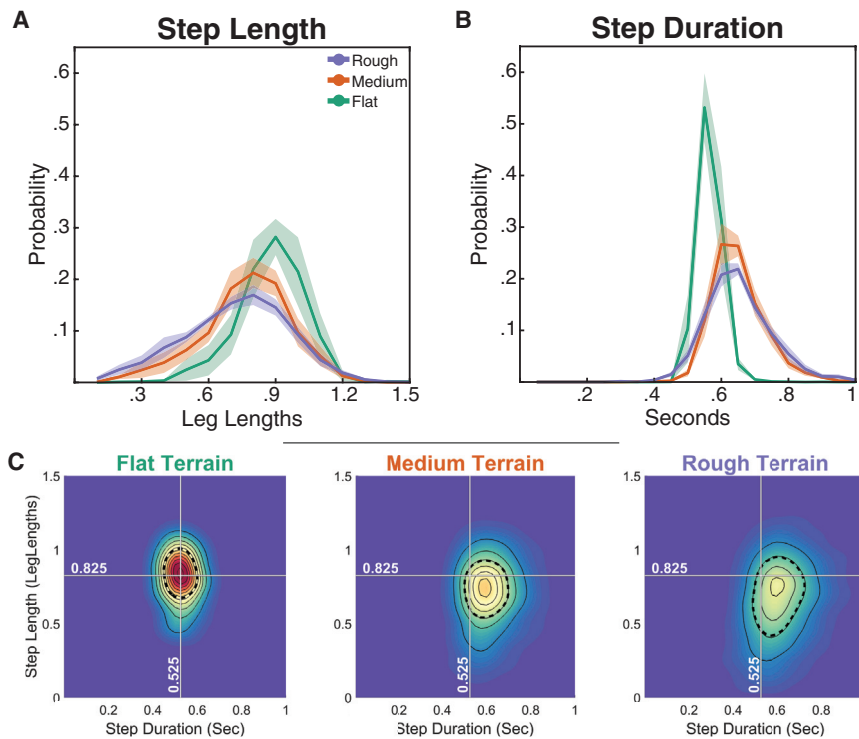
A Step Length

B Step Duration

Figure 2. Step Length and Duration in the Three Terrains

(A and B) Step length (A) and duration (B) in the different terrains. Thick lines are means across subjects; shaded regions show ± SEM; bin sizes are 0.1 leg lengths and 50 ms, respectively.

(C) Density map of the relationship between step length and duration for individual steps in the Flat, Medium, and Rough conditions. White crosshairs show the peak step length (.825 leg lengths) and duration (.525 s) in the Flat terrain, which represents subjects' preferred gait parameters. Although the distributions in the Medium and Rough are more diffuse, the peaks remain close to that shown for the Flat terrain.

C

RESULTS

We used a Positive Science mobile eye tracker and a Motion Shadow inertial measurement unit (IMU)-based motion-capture system to record the gaze and full-body kinematics of subjects as they walked over three types of terrain (Figure 1A; Video S1; see STAR Methods for details)—an extremely rocky dry creek bed (Rough terrain, Video S2), a moderately rocky trail (Medium terrain), and a flat packed-earth trail (Flat terrain). Examining the relationship between gaze and footholds in these terrains elucidates the dynamic trade-off between different locomotor constraints (Figures 1B–1E). The Rough terrain condition consisted mostly of large rocks capable of supporting a subject's weight so that traversing that terrain required placing the feet onto the limited number of stable regions atop the rocks that comprised the path. In contrast, the Medium terrain was composed of smaller rocks that were too small to support a person's weight, so locomotion required placing the feet in the stable regions between these potential impediments. The Flat terrain was a packed-earth trail that was largely free of any obstacles that might interfere with the placement of the feet. The Medium and Rough terrains required subjects to visually identify the locations of safe footholds and adjust their gait cycle appropriately for the layout of the upcoming terrain. In contrast, in the Flat terrain walkers could adopt their energetically optimal preferred gait cycle while occasionally scanning the upcoming path for potential hazards.

Influence of Terrain on the Gait Cycle

Humans walkers in unconstrained environments adopt a preferred walking speed characterized by a combination of step length and step duration that minimizes the energetic cost

of transport [8, 26–29]. Our data are consistent with this observation: in the Flat terrain, subjects selected a mean walking speed of 1.38 ± 0.05 m/s with a highly regular relationship between step length and duration, indicative of an energetically optimized gait cycle (Figure 2, green lines). In contrast, subjects walked more slowly in the Medium and Rough conditions (.98 ± .03 m/s and 0.88 ± .06 m/s, respectively; see table in Quantification and Statistical Analysis, row 1 for statistics), and their steps became shorter, slower, and more variable (Figures 2A and 2B; see table in Quantification and Statistical Analysis, rows 2 and 3). Subjects maintained a somewhat regular step length/duration pairing but displayed increased variability in these parameters (Figure 2C; see table in Quantification and Statistical Analysis, row 4). Because walkers were free to adopt their preferred gait cycle in the Flat terrain, the deviation from this pattern in the Medium and Rough terrains represents a trade-off between the most energetically optimal combination of gait parameters and need to alter footholds to maintain stability in the more difficult terrains. However, despite the increased variability, there were still distinct peaks in the distribution of walkers' step parameters in the Medium and Rough terrains. It seems that despite the additional demands afforded by the more difficult terrains, walkers still attempt to maintain a regular relationship between step length and duration similar to that selected in the Flat terrain (Figure 2C). To understand the role that vision played in this trade-off between efficiency and stability, we look to the variations in walkers' gaze behavior in the different terrains.

Gaze Allocation in the Different Terrains

Analysis of gaze behavior in the different terrains reveals the way subjects gather the information needed to adapt their gait cycle to the layout of the upcoming path. The most immediate effect of the different terrains was the amount of time subjects looked at the ground in front of them as opposed to more distant locations. In the Flat terrain, subjects' gaze intersected the ground plane within 4 leg lengths of their current position about half of the time, whereas nearly all of each subject's gaze was directed toward the ground in the Medium and Rough terrains (58.0 ± 10%,
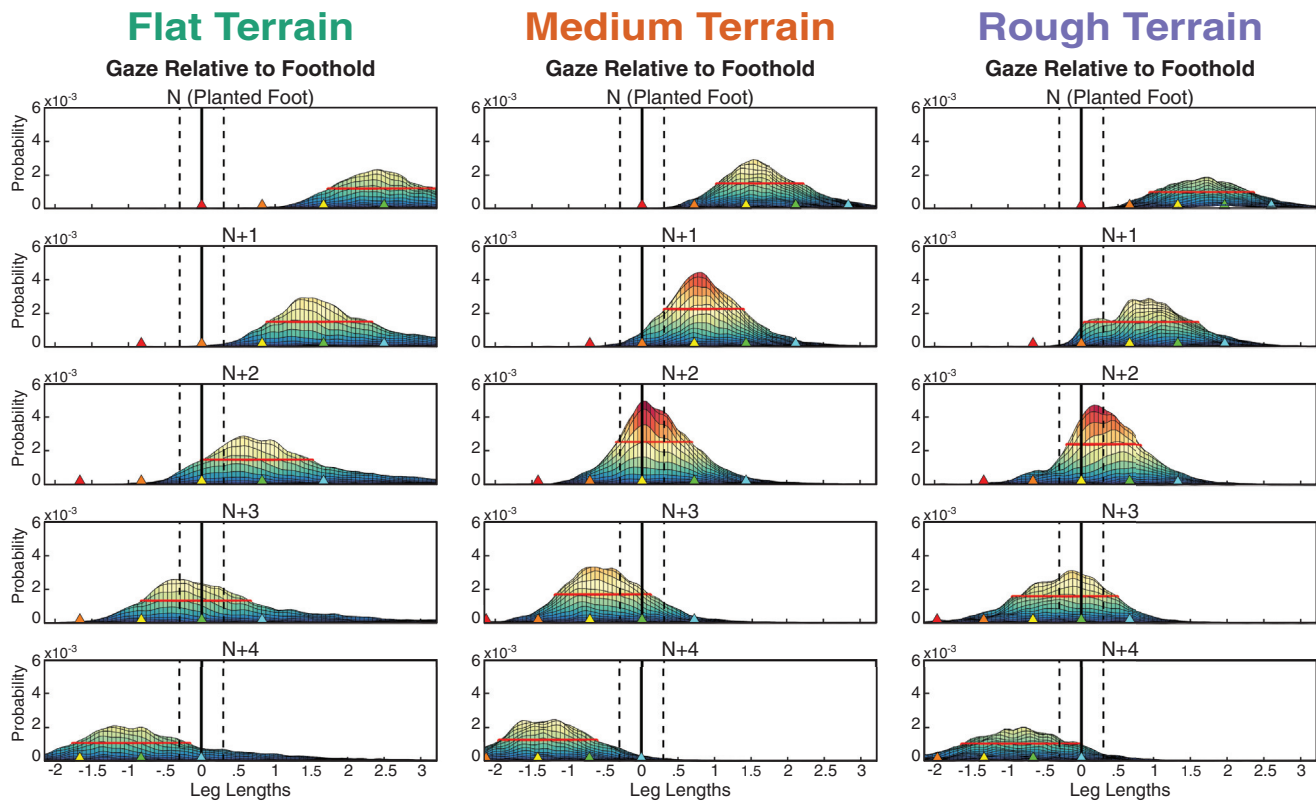
Figure 3. Gaze Density in Different Foothold-Centered Reference Frames in the Three Terrains

Gaze density in different foothold-centered reference frames for the different terrain. The plots are cross-sections of the 2D distributions along the locomotor axis. The top row shows the distribution of gaze-groundplane intersections when plotted relative to the foot that was planted at the time that the intersection was recorded (Foothold N [planted foot], red triangle). Subsequent rows show gaze density when plotted relative to steps that were upcoming at the time the gaze-ground intersection was recorded (Footholds N+1 – N+4, orange, yellow, green, and cyan triangles). Vertical dotted lines show ± 0.3 leg lengths, which was the area used in the analysis shown in Figure 4B. Horizontal red line shows the half-maximum height. This figure shows mean gaze distribution for all six subjects, but all later analyses were based on individual subject's gaze distribution (see also Figure S1A for a 2D heatmap version of this figure and Figures S2–S7 for individual subject data).

94.3 ± 1%, 96.0 ± 1%, respectively; see table in Quantification and Statistical Analysis, rows 5–8). More importantly, the nature of the linkage between gaze and gait varied substantially in the different terrains.

Gaze Coupling to Upcoming Footholds

If the increased time spent looking at the ground in the Medium and Rough terrains was driven by step planning, then the distribution of gaze on the ground should be linked to the locations of future footholds. To calculate the density of the subjects' gaze position relative to upcoming footholds, we first calculated the intersections between the 3D gaze vector and a 2D ground plane located at the same height as the heel marker of the subject's planted foot. This intersection point was initially measured in world-centered coordinates, with the origin set at the start position. To situate these data in a foothold-centered reference frame, we subtracted the position of the heel marker on the planted foot from each of the gaze-ground intersection points that were recorded during that step in order to situate them in a reference frame centered on the planted foot. That is, for each frame of the recording, we took the (x,y) location of the intersection between the gaze vector and the ground plane

and subtracted the (x,y) location of the foot that was planted on that frame (see STAR Methods).

The gaze probability distribution relative to the planted foot indicates that subjects spend most of their time in each of the terrains looking at the ground roughly two to four steps ahead (Foothold N, Figure 3, first row). However, if subjects fixate the locations of their upcoming footholds in the Medium and Rough terrains, then some of the spread of the distribution of gaze on the ground will be related to variability in the footholds themselves. To examine this source of variability, we re-centered each gaze point on the locations of upcoming footholds. Rather than plotting gaze relative to the location of the planted foot (Foothold N), gaze location was plotted relative to the location where the foot was going to be placed (N+1) or to the footholds that were coming up after that (N+2, N+3, and N+4), as shown in the different rows in Figure 3. That is, rather than subtracting the location of the planted foot from the location of each gaze/ground intersection, we subtracted the location of the footholds that were coming up at the time that the gaze/ground intersection was recorded.

Plotting gaze relative to future footholds reveals that gaze was most tightly clustered around the second upcoming foothold in
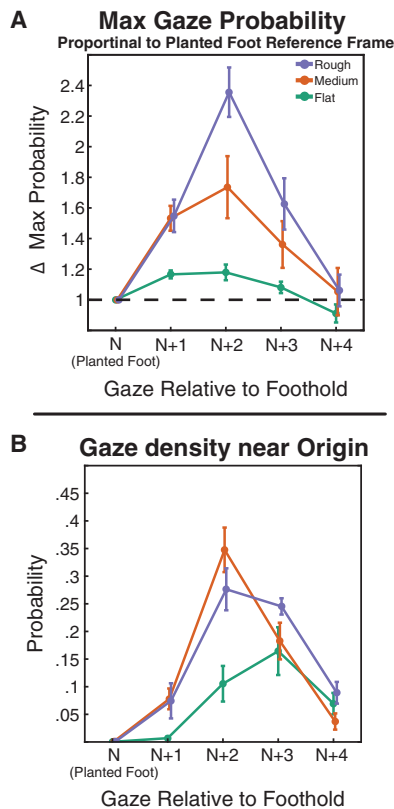
A

Max Gaze Probability
Proportinal to Planted Foot Reference Frame

B

Gaze density near Origin

Figure 4. Change in Maximum Gaze Probability and Sum Gaze Density near the Origin

(A) The change in the maximum value of the gaze probability distributions in the different foothold-centered reference frames shown in the rows of Figure 3. Each value was normalized by the maximum value of the distribution in the Foothold N (planted Foot) reference frame.

(B) The sum of the probability distribution within ± 0.3 leg lengths of the origin (dotted vertical lines in Figure 3) for each foothold-centered reference frame. Dots show subject means; error bars are ± 1 SEM. See also Figure S1B for a measure of spread in the gaze probability distributions. See also Figures S2–S7.

the Medium and Rough terrains (Figure 3, third row). We quantified this clustering by analyzing two features of a probability density: the peak and spread. The change in the peak is shown in Figure 4A, which plots the change in magnitude of the peak of the distribution relative to that at Foothold N for the different terrains (see Figure S1B for analysis of spread). When gaze is plotted relative to Foothold N+2, the peak increased by a factor of 2.36 for the Rough terrain and 1.74 in the Medium terrain (see table in Quantification and Statistical Analysis, rows 9 and 10). In contrast, in the Flat terrain, plotting gaze relative to upcoming footholds had comparatively little effect on the gaze distribution (1.18 increase for N+2; see table in Quantification and Statistical Analysis, row 11). This result suggests that gaze was strongly coupled to the locations of upcoming footholds in the Rough and Medium terrains, indicating that subjects fixated the precise locations of upcoming footholds several steps in advance. This was not the case in the Flat terrain. In that condition, when subjects looked at the ground, they did not preferentially fixate the locations where they would soon put their feet. As a result, subtracting the variability of upcoming steps from the gaze probability distribution had a minimal effect on its density, in comparison to the terrains where foot placement had a more substantial visual component.

Probability of Looking at Each Foothold

To reveal the relative importance of each future foothold for visual planning in the different terrains, we directly compared how much time subjects spent looking at specific footholds. To accomplish this, we integrated the gaze density in the region closest to the location of upcoming foot placement (area within the vertical black dotted lines of Figure 3). The proportion of time that subjects' gaze was near the location of each upcoming foothold is shown in Figure 4B. This plot reveals that in the Medium terrain subjects directed most of their gaze toward Foothold N+2 (34.8 ± 4%), with substantially less directed toward N+3 (18.3 ± 3%; see table in Quantification and Statistical Analysis, row 12). However, in the Rough terrain, subjects split gaze evenly between N+2 and N+3 (27.6 ± 4% and 24.5 ± 1%, respectively; see table in Quantification and Statistical Analysis, row 13). The preponderance of gaze on Foothold N+2 matches the predictions of lab-based studies, which showed that providing walkers with visual information from two steps ahead allowed them to accurately control foot placement while exploiting their inverted pendulum dynamics as well as they do with unconstrained vision [21, 22, 25]. These results suggest that walkers plan two steps ahead in order to maintain their momentum between subsequent steps and avoid the costly muscular intervention needed to redirect the body within a step. Subjects do occasionally look at Foothold N+1 in the Medium and Rough terrains, suggesting that locomotion over real-world terrain relies on a combination of visual-feedback-driven control of the step to Foothold N+1 [30] as well as feedforward planning of upcoming steps (Footholds N+2 and beyond).

Path Planning in the Different Terrains

The tendency to split gaze between N+2 and N+3 in the Rough terrain may arise from the greater need for path planning in that environment. In the Medium terrain, subjects were likely to find a safe foothold without deviating far from their locomotor trajectory (note that this was also the case in the environments used in [21, 22]). However, the Rough terrain was constrained enough that a walker would need to ensure that their current plan for Foothold N+2 wouldn't carry them toward a region with no good options for Foothold N+3.

In line with this explanation, subjects' gaze behavior in the Rough terrain showed substantially more spread in the mediolateral dimension than the Medium or Flat terrains. In the Rough terrain, the mediolateral spread at half-maximum of the gaze probability distribution in the planted foot (Foothold N) reference frame was 1.05 ± .22 leg lengths. In the Medium and Flat terrains, the mediolateral spread was 0.79 ± .26 and 0.44 ± .06 leg lengths, respectively. In contrast, the anterior-posterior spread at half-max was similar for all terrains (1.32 ± .33, 1.16 ± .35, 1.24 ± .32) leg lengths for Flat, Medium, and Rough (see top row of Figure S1A). This difference suggests an increased need to search for viable footholds off of the primary locomotor axis in the Rough terrain.

Analysis of path variability supports the idea that the fixations on Foothold N+3 are related to the increased importance of path
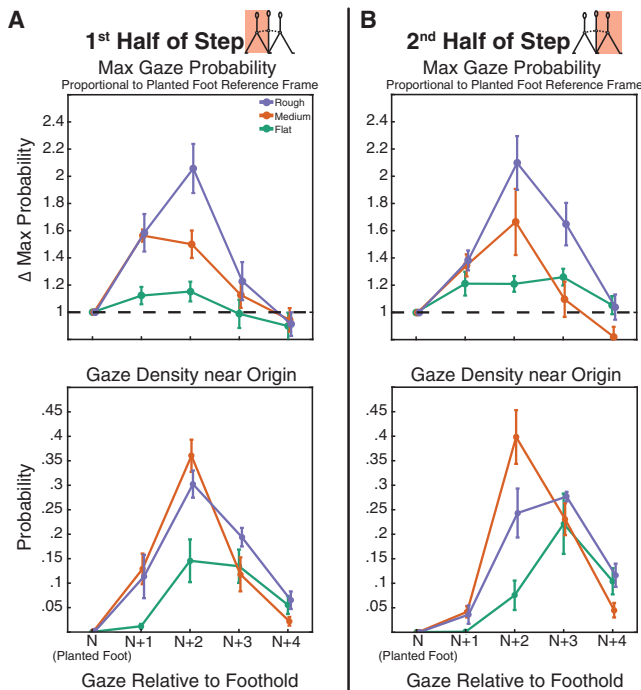
Figure 5. Changes in Gaze/Foothold Relationship in the Early and Latter Halves of Steps

(A and B) Changes in subjects' gaze probability distribution during the first and second half of each step in the different terrains ([A] and [B], respectively). Steps were defined as the period between heelstrike on a given foothold and the frame prior to subsequent heelstrike. Other than the separation of data according to the gait cycle, the max-probability and sum-probability analyses are the same as those shown in Figure 4.

planning in the Rough terrain. We computed a path straightness index by taking the ratio of the straight-line distance between the start and end points of each path and the actual distance traveled by subjects COM as they traveled between these points [31]. This ratio (always between 0 and 1) showed that subjects followed comparably straight walking paths in the Flat and Medium terrain conditions (mean path straightness 0.86 ± .02 and 0.82 ± .02, respectively), but walking trajectories in the Rough terrain were notably more tortuous (mean path straightness 0.59 ± .01; see table in Quantification and Statistical Analysis, rows 14–17). Subjects' deviation from the minimum-distance path reveals another trade-off between the energetically efficient straight-line path and the need to place the feet on stable locations.

Time-Course of Gaze Relative to Gait Cycle

If subjects' propensity to look toward Foothold N+3 in the Rough terrain is related to path planning, then we should expect to see some variation in the timing of their gaze behavior within the gait cycle. Specifically, subjects should identify a viable location for Foothold N+2 prior to midstance (in time for the critical control phase [25]) and then look ahead to ensure that their chosen foothold would allow them to reach a viable Foothold N+3. Examination of the time course of gaze density during the course of a step is consistent with this hypothesis. Figure 5 shows the analyses

from Figure 4 separated into the first and second half of each step (with steps beginning at heelstrike of the planed foot and ending one frame prior to heelstrike of the next step). During the first half of each step, subjects' gaze in both the Medium and Rough terrains is primarily located in the area around the upcoming Foothold N+2. In the latter half of the step, the Rough-terrain gaze density is split equally between N+2 and N+3, whereas the Medium terrain remains centered on N+2 (see table in Quantification and Statistical Analysis, rows 18–21). Thus, the tendency to split gaze between Footholds N+2 and N+3 in the Rough—but not Medium—terrain shows that subjects' gaze-allocation strategies were not only tuned to whether or not foot placement required visual guidance (i.e., Flat versus Medium and Rough) but also to the variations in the specific task demands afforded by the Medium and Rough terrains.

The density of gaze around Foothold N+3 in the Flat terrain may also be a hallmark of the minor amount of path planning that was necessary in that terrain. Although subjects did not fixate the locations of upcoming footholds in that condition (Figures 3 and 4), their gaze behavior showed a similar shift toward the region near foothold N+3 in the latter half of steps to the one seen in the Rough terrain. The flat terrain was regular enough that individual footholds did not require visual identification as they did in the more difficult conditions. However, the path was not completely free from potential hazards—small branches, piles of leaves, and loose rocks were occasionally present on this packed-earth trail. If a walker identified one of these potential impediments far enough in advance, they could steer around it with only small alterations of the preceding steps [20, 32, 33]. This similarity between the Flat and Rough terrain highlights the fact that locomotor behaviors in these very different environments are not categorically different from each other. Rather, they exist on a continuum wherein behavior emerges from the interaction of locomotor goals with the complexity of the terrain being traversed.

Temporal versus Spatial Look-Ahead

Despite the distinct differences between gaze behavior in the different terrains, subjects maintained a constant temporal look-ahead in all three conditions. We analyzed subjects' point of gaze on the ground relative to the position of their COM, discarding frames where gaze was not within 0.5 leg lengths of their future COM trajectory. Spatial look-ahead was calculated as the Euclidean distance between their point of gaze and their current COM position, while temporal look-ahead was defined as the time that would elapse until the subject reached that point. Although there was a substantial difference between look-ahead distance in the Flat terrain compared to the Medium and Rough terrains (Figure 6A; see table in Quantification and Statistical Analysis, rows 22–25), subjects maintained a constant *temporal* look in all three terrains (Figure 6B; see table in Quantification and Statistical Analysis, rows 26–29). That is, although subjects walking in the Flat terrain looked at the ground less frequently and did not fixate on footholds as they did in the more difficult terrains, when they did look at the ground, they directed their gaze toward regions of the upcoming path that they would reach within a similar time period to the fixated footholds in the Medium and Rough terrains. Given the differences in walking speed between the different
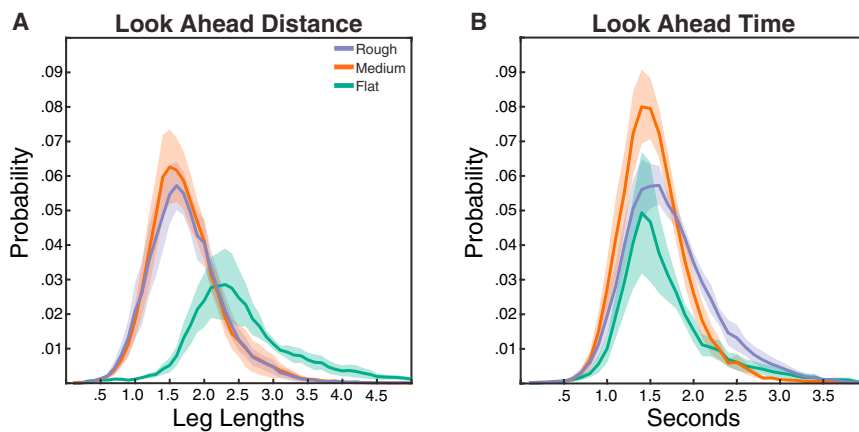
Figure 6. Look-Ahead Distance and Look-Ahead Time in the Three Terrains

(A) Distribution of subject look-ahead distances for each of the terrain conditions. Look-ahead distance was calculated as the distance between subjects' center of mass and gaze-groundplane intersections on frames where gaze was within 0.5 leg lengths of the walking path. The data presented in this figure are similar to data shown in the top row of Figure 3.

(B) Distribution of look-ahead times in each terrain condition. On every frame where gaze was within 0.5 leg lengths of the walking path, look-ahead time was defined as the time that would elapse before the subject would reach the point on their walking trajectory nearest to their point of gaze. Solid lines show the mean across subjects; shaded region is ± 1 SEM; bin sizes 0.1 leg lengths for (A) and 100 ms for (B). Note that the distributions were normalized by trial duration and do not include frames where the subject was not looking within 0.5 leg lengths of the path. As such, each distribution sums to the proportion of the time that the subject's gaze was near their walking path (.41 ± .16, 0.69 ± .06, 0.66 ± .08 for Flat, Medium, and Rough, respectively).

conditions, subjects must have scaled their look-ahead distance in order to ensure that they would always have a consistent degree of certainty about the upcoming path over the next 1.5 s.

DISCUSSION

We measured full-body kinematics and eye movements during locomotion through the natural world and found a coupling between human eye movements and the gait cycle that varied with the difficulty of the terrain being traversed. These observations reveal the inextricable role of gaze in human walking and the ways that this relationship is tightly linked to momentary informational demands of the locomotor task. The low variability between subjects is particularly interesting, considering that participants received no instructions for how to complete this task, other than to walk from the start position to the end point while maintaining a comfortable walking speed (see Figures S2–S7 for individual subject data). This consistency suggests that each subject's gaze behavior emerged primarily from the constraints of the locomotor task and the need to adapt energetically optimal preferred gait cycle to the complexity of the terrain being traversed.

The basic locomotor task does not change as a walker traverses different types of terrain; in each case, the subject's goal was to use their legs to move their body from the start location to the end location. However, the information needed to complete that task varies dramatically in different environments, and subjects showed distinct gaze-allocation strategies for each of the three types of terrains.

The role of vision in Flat terrain is modest. In that condition, subjects only looked at the ground about half of the time, and gaze was only loosely related to upcoming footholds. This is consistent with Pelz and Rothkopf's [11] finding that gaze fell on a dirt path 62% of the time and on a paved walkway only 36% of the time. 't Hart and Einhäuser [13] also noted that gaze was generally higher in the visual field when walking on roadway versus steps. In contrast, nearly all of the subjects' gaze was on the upcoming path in the Medium and Rough terrains and was tightly coupled with upcoming footholds (Figure 4). Specifically, gaze in those terrains was coupled to Foothold N+2, which is indicative of a visual control strategy that seeks to approximate the energetic efficiency of flat, obstacle-free environments [21–25]. However, the limited number of viable footholds in the rough terrain introduced an additional need for longer-term planning. In response, walkers maintained the energetically efficient foot-placement strategy of the Medium terrain but split their gaze more evenly between Foothold N+2 and N+3. Interestingly, the gaze distribution peaked at Foothold N+2 early in the gait cycle, which ensured that a foothold could be found in time for the critical phase for the visual control of foot placement [25], before shifting to N+3 later in the step.

However, despite the variations in gaze behavior between environments, subjects maintained a constant look-ahead time of roughly 1.5 s in all of the terrain conditions. Until this point, most of our discussion has focused on the biomechanical elements that shape the visual control of foot placement (e.g., [24, 25]). However, the fact that temporal look ahead in the Flat terrain (where foot placement did not require precise visual guidance) was similar to the more difficult terrains suggests that there may be other factors underlying this 1.5 s look-ahead window. A similar look-ahead time has been observed in stair-climbing [34] and also in driving [35–37]. In addition, in the domain of upper-limb movements, it has been demonstrated that spontaneous look-ahead fixations in preparation for an upcoming reach typically occur about 2 s ahead of the reaching movement [38]. Considering its prevalence across this wide range of motor actions, it is possible that this timescale represents a fundamental limitation of visual memory, whereby the rate of decay entails that precision movements are best guided by information that is less than 2 s old. If so, then subjects' gaze behavior during locomotion may be operating under the same kind of just-in-time strategy that has been observed in other visuomotor tasks [39, 40].

Whatever its underlying source, the constant look-ahead times in the three terrains suggest that walkers are maintaining some sort of global locomotor strategy that is being tuned to the environment they are traversing. Specifically, walkers seem

to deploy their gaze so as to ensure that they maintain some degree of certainty over what will happen in the next 1.5–2 s. Such a strategy would explain why subjects need to slow down when traversing the more difficult terrains. There is nothing about the physical movements associated with locomotion in difficult terrain that requires slower execution, but rather the slower speeds may represent the maximum rate that subjects are capable of gathering the information needed to support locomotion in the face of the higher uncertainty of the Medium and Rough terrains. That is, the ability to gather information about the upcoming path may be the bottleneck that determines a walker's maximum walking speed on the different terrains.

Behavior in the natural world is an information problem—actors must reduce their uncertainty about the aspects of the world that are relevant to a given task to a level that will allow for successful performance [41–43]. Recent approaches to the control of movement define optimal behavior as the minimization of a cost function derived from sensory noise, environmental uncertainty, and the specific requirements of the task at hand [41, 44]. In the context of statistical decision theory, an optimal agent will direct gaze in a way that minimizes the uncertainty of variables necessary to complete a given task [45, 46], and it has been shown that gaze-control strategies in many contexts are shaped by the informational requirements of the task being performed [13, 42, 43, 47–50]. Good action decisions require not only good sensory data but also a consideration of the costs and benefits of the action. Indeed, recent work reveals an intimate relation between the neural control of gaze and the underlying dopaminergic reward machinery [51–54].

The present results reveal that this decision-theoretic framework may also shed light on the control of locomotion in natural environments. That is, the terrain-tuned gaze-allocation strategies and the global 1.5 s look-ahead time may emerge from a global optimization of all the relevant factors associated with walking over the terrains tested in this study. On one hand, human walkers seek to minimize their energetic cost of transport by adopting their preferred gait cycle ([27, 29]). However, when the terrain becomes more complex, they deviate from energetically optimal movement pattern without abandoning it entirely (Figure 2). The biomechanics of bipedal gait entail that the cost deviating from the preferred gait cycle may be minimized by planning two steps ahead ([25]; Figure 4A), but when the terrain requires significant path planning, walkers will look ahead to the third upcoming foothold earlier in the gait cycle (Figures 4B and 5). This planning window may reflect limitations in working memory, but it also may represent some optimum for path planning as it has been shown that planning future steps yields diminishing returns after about two to three steps [55–58].

By deploying gaze in a manner that is tuned to the complexity of the terrain being traversed, walkers can ensure that they always have enough certainty about the layout of the coming path to commit the momentum of their body to a newly planted foot. In flat environments, the regularity of the terrain means that this certainty can be achieved by only occasional glances at the upcoming path. In rough terrain, achieving a similar degree of confidence is a more arduous process. Thus, the way that vision is deployed for the control of locomotion reveals the underlying structure of the sensorimotor decisions that support successful performance in the face of the complex and varying demands of the natural world.

STAR★METHODS

Detailed methods are provided in the online version of this paper and include the following:

- KEY RESOURCES TABLE
- CONTACT FOR RESOURCE SHARING
- EXPERIMENTAL MODEL AND SUBJECT DETAILS
- METHOD DETAILS
  - Equipment
  - Experimental Task
  - Experimental Protocol
  - VOR-based calibration and data post-processing
  - Ground plane estimation
  - Reference frame definition
  - Sensor alignment correction
  - Calibration error and validation
  - Known sources of measurement error
- QUANTIFICATION AND STATISTICAL ANALYSIS
  - Calculating gaze density
  - Statistics
- DATA AND SOFTWARE AVAILABILITY

REFERENCES

1. Lovejoy, C.O., Suwa, G., Spurlock, L., Asfaw, B., and White, T.D. (2009). The pelvis and femur of *Ardipithecus ramidus*: the emergence of upright walking. Science *326*, 71–71.e6.

2. Georgopoulos, A., and Grillner, S. (1989). Visuomotor coordination in reaching and locomotion. Science *245*, 1209–1210.

3. Tucker, V.A. (1975). The energetic cost of moving about. Am. Sci. *63*, 413–419.

4. Hunt, K.D. (1994). The evolution of human bipedality: ecology and functional morphology. J. Hum. Evol. 26, 183–202.

5. Holt, K.J., Jeng, S.F., Rr, R.R., and Hamill, J. (1995). Energetic cost and stability during human walking at the preferred stride frequency. J. Mot. Behav. 27, 164–178.

6. Kuo, A.D. (2001). A simple model of bipedal walking predicts the preferred speed-step length relationship. J. Biomech. Eng. 123, 264–269.

7. Kuo, A.D. (2007). The six determinants of gait and the inverted pendulum analogy: A dynamic walking perspective. Hum. Mov. Sci. 26, 617–656.

8. Finley, J.M., Bastian, A.J., and Gottschall, J.S. (2013). Learning to be economical: the energy cost of walking tracks motor adaptation. J. Physiol. 591, 1081–1095.

9. Selinger, J.C., O'Connor, S.M., Wong, J.D., and Donelan, J.M. (2015). Humans can continuously optimize energetic cost during walking. Curr. Biol. 25, 2452–2456.

10. Wong, J.D., O'Connor, S.M., Selinger, J.C., and Donelan, J.M. (2017). Contribution of blood oxygen and carbon dioxide sensing to the energetic optimization of human walking. J. Neurophysiol. 118, 1425–1433.

11. Pelz, J.B., and Rothkopf, C. (2007). Oculomotor Behavior in Natural and Man-Made. In Eye Movements: A Window on Mind and Brain, R.P.G. van Gompel, M.H. Fischer, W.S. Murray, and R.L. Hill, eds. (Oxford: Elsevier), pp. 661–676.

12. Foulsham, T., Walker, E., and Kingstone, A. (2011). The where, what and when of gaze allocation in the lab and the natural environment. Vision Res. 51, 1920–1931.

13. 't Hart, B.M., Schmidt, H.C.E.F., Klein-Harmeyer, I., and Einhäuser, W. (2013). Attention in natural scenes: contrast affects rapid visual processing and fixations alike. Philos. Trans. R. Soc. Lond. B Biol. Sci. 368, 20130067.

14. 't Hart, B.M., Schmidt, H.C.E.F., Roth, C., and Einhäuser, W. (2013). Fixations on objects in natural scenes: dissociating importance from salience. Front. Psychol. 4, 455.

15. Hollands, M.A., Marple-Horvat, D.E., Henkes, S., and Rowan, A.K. (1995). Human eye movements during visually guided stepping. J. Mot. Behav. 27, 155–163.

16. Hollands, M.A., and Marple-Horvat, D.E. (2001). Coordination of eye and leg movements during visually guided stepping. J. Mot. Behav. 33, 205–216.

17. Patla, A.E., and Vickers, J.N. (1997). Where and when do we look as we approach and step over an obstacle in the travel path? Neuroreport 8, 3661–3665.

18. Marigold, D.S., and Patla, A.E. (2007). Gaze fixation patterns for negotiating complex ground terrain. Neuroscience 144, 302–313.

19. Patla, A.E. (1998). How is human gait controled by vision? Ecol. Psychol. 10, 287–302.

20. Moraes, R., Lewis, M.A., and Patla, A.E. (2004). Strategies and determinants for selection of alternate foot placement during human locomotion: influence of spatial and temporal constraints. Exp. Brain Res. 159, 1–13.

21. Matthis, J.S., and Fajen, B.R. (2014). Visual control of foot placement when walking over complex terrain. J. Exp. Psychol. Hum. Percept. Perform. 40, 106–115.

22. Matthis, J.S., and Fajen, B.R. (2013). Humans exploit the biomechanics of bipedal gait during visually guided walking over complex terrain. Proc. Biol. Sci. 280, 20130700.

23. Matthis, J.S., Barton, S.L., and Fajen, B.R. (2015). The biomechanics of walking shape the use of visual information during locomotion over complex terrain. J. Vis. 15, 10.

24. Barton, S.L., Matthis, J.S., and Fajen, B.R. (2017). Visual regulation of gait: Zeroing in on a solution to the complex terrain problem. J. Exp. Psychol. Hum. Percept. Perform. 43, 1773–1790.

25. Matthis, J.S., Barton, S.L., and Fajen, B.R. (2017). The critical phase for visual control of human walking over complex terrain. Proc. Natl. Acad. Sci. USA 114, E6720–E6729.

26. Bertram, J.E., and Ruina, A. (2001). Multiple walking speed-frequency relations are predicted by constrained optimization. J. Theor. Biol. 209, 445–453.

27. Zarrugh, M.Y., Todd, F.N., and Ralston, H.J. (1974). Optimization of energy expenditure during level walking. Eur. J. Appl. Physiol. Occup. Physiol. 33, 293–306.

28. Minetti, A.E., Capelli, C., Zamparo, P., di Prampero, P.E., and Saibene, F. (1995). Effects of stride frequency on mechanical power and energy expenditure of walking. Med. Sci. Sports Exerc. 27, 1194–1202.

29. Ralston, H.J. (1958). Energy-speed relation and optimal speed during level walking. Int. Zeitschrift für Angew. Physiol. Einschl. Arbeitsphysiologie 17, 277–283.

30. Reynolds, R.F., and Day, B.L. (2005). Visual guidance of the human foot during a step. J. Physiol. 569, 677–684.

31. Benhamou, S. (2004). How to reliably estimate the tortuosity of an animal's path: straightness, sinuosity, or fractal dimension? J. Theor. Biol. 229, 209–220.

32. Lee, D.N., Lishman, J.R., and Thomson, J.A. (1982). Regulation of gait in long jumping. J. Exp. Psychol. Hum. Percept. Perform. 8, 448–459.

33. de Rugy, A., Taga, G., Montagne, G., Buekers, M.J., and Laurent, M. (2002). Perception–action coupling model for human locomotor pointing. Biol. Cybern. 87, 141–150.

34. Zietz, D., and Hollands, M. (2009). Gaze behavior of young and older adults during stair walking. J. Mot. Behav. 41, 357–365.

35. Land, M.F., and Lee, D.N. (1994). Where we look when we steer. Nature 369, 742–744.

36. Land, M.F. (1998). The visual control of steering. In Vision and Action, L.R. Harris, and M. Jenkin, eds. (Cambridge: Cambridge University Press), pp. 163–180.

37. Land, M.F., and Tatler, B.W. (2001). Steering with the head. the visual strategy of a racing driver. Curr. Biol. 11, 1215–1220.

38. Mennie, N., Hayhoe, M., and Sullivan, B. (2007). Look-ahead fixations: anticipatory eye movements in natural tasks. Exp. Brain Res. 179, 427–442.

39. Johansson, R.S., Westling, G., Bäckström, A., and Flanagan, J.R. (2001). Eye-hand coordination in object manipulation. J. Neurosci. 21, 6917–6932.

40. Pelz, J., Hayhoe, M., and Loeber, R. (2001). The coordination of eye, head, and hand movements in a natural task. Exp. Brain Res. 139, 266–277.

41. Maloney, L.T., and Zhang, H. (2010). Decision-theoretic models of visual perception and action. Vision Res. 50, 2362–2374.

42. Hayhoe, M., and Ballard, D. (2005). Eye movements in natural behavior. Trends Cogn. Sci. 9, 188–194.

43. Maeda, R.S., O'Connor, S.M., Donelan, J.M., and Marigold, D.S. (2016). Foot placement relies on state estimation during visually guided walking. J Neurophysiol. 117, 480–491.

44. Wolpert, D.M., and Landy, M.S. (2012). Motor control is decision-making. Curr. Opin. Neurobiol. 22, 996–1003.

45. Sims, C.R., Jacobs, R.A., and Knill, D.C. (2011). Adaptive allocation of vision under competing task demands. J. Neurosci. 31, 928–943.

46. Hayhoe, M., and Ballard, D. (2014). Modeling task control of eye movements. Curr. Biol. 24, R622–R628.

47. Tatler, B.W., Hayhoe, M.M., Land, M.F., and Ballard, D.H. (2011). Eye guidance in natural vision: reinterpreting salience. J. Vis. 11, 5.

48. Land, M.F. (2004). The coordination of rotations of the eyes, head and trunk in saccadic turns produced in natural situations. Exp. Brain Res. 159, 151–160.

49. Corbetta, M., Kincade, J.M., Ollinger, J.M., McAvoy, M.P., and Shulman, G.L. (2000). Voluntary orienting is dissociated from target detection in human posterior parietal cortex. Nat. Neurosci. 3, 292–297.

50. Franchak, J.M., and Adolph, K.E. (2010). Visually guided navigation: head-mounted eye-tracking of natural locomotion in children and adults. Vision Res. 50, 2766–2774.

51. Gottlieb, J. (2017). Understanding active sampling strategies: Empirical approaches and implications for attention and decision research. Cortex. https://doi.org/10.1016/j.cortex.2017.08.019.

52. Gottlieb, J. (2012). Attention, learning, and the value of information. Neuron 76, 281–295.

53. Platt, M.L., and Glimcher, P.W. (1999). Neural correlates of decision variables in parietal cortex. Nature 400, 233–238.

54. Yasuda, M., Yamamoto, S., and Hikosaka, O. (2012). Robust representation of stable object values in the oculomotor Basal Ganglia. J. Neurosci. 32, 16917–16932.

55. Zaytsev, P., Hasaneini, S.J., and Ruina, A. (2015). Two steps is enough: no need to plan far ahead for walking balance. In Proceedings of the 2015 IEEE International Conference on Robotics and Automation, pp. 6295–6300.

56. Koolen, I.T., De Boer, T., Rebula, J., Goswami, A., and Pratt, J. (2012). Capturability-based analysis and control of legged locomotion, part 1: theory and application to three simple gait models. Intl J Rob Res. 31, 1094–1113.

57. Pratt, J., Koolen, T., De Boer, T., Rebula, J., Cotton, S., Carff, J., Johnson, M., and Neuhaus, P. (2012). Capturability-based analysis and control of legged locomotion, part 2: application to M2V2, a lower-body humaoid. Intl J Rob Res. 31, 1117–1133.

58. Zaytsev, P., Wolfslag, W., and Ruina, A. (2018). The boundaries of walking stability: viability and controllability of simple models. Trans. Robot. PP, 1–17.

59. Evans, K.M., Jacobs, R.a, Tarduno, J.a, and Pelz, J.B. (2012). Collecting and analyzing eye-tracking data in outdoor environments. J. Eye Mov. Res. 5, 1–19.

60. Roetenberg, D., Luinge, H., and Slycke, P. (2009). Xsens MVN : full 6DOF human motion tracking using miniature inertial sensors. Hand (NY), 10.1.1.569.9604.

STAR★METHODS

KEY RESOURCES TABLE

REAGENT or RESOURCE	SOURCE	IDENTIFIER
Deposited Data		
Raw and post-processed data, and MATLAB code	This paper	https://doi.org/10.6084/m9.figshare.6130850
Software and Algorithms		
Yarbus eye-tracking software	Positive Science	Positivescience.com
Motion Shadow IMU-based motion capture software	Motion Shadow	Motionshadow.com
MATLAB	MathWorks	Mathworks.com

CONTACT FOR RESOURCE SHARING

Further information and requests for resources no already available should be directed to and will be fulfilled by the Lead Contact, Jonathan Samir Matthis (matthis@utexas.edu).

EXPERIMENTAL MODEL AND SUBJECT DETAILS

Six human subjects participated in this experiment (2 female, 4 male, mean age: 26.8 ± 4 years mean height: 1.77 ± .1 m, mean weight: 76.2 ± 26kg, mean leg length: 0.93 ± .07 m). Subjects signed informed consent prior to participating in the experiment, and all activities were approved by the Institutional Review Board at the University of Texas at Austin.

METHOD DETAILS

Equipment
Subjects' gaze was tracked using a Positive Science monocular mobile eye tracker recording at 30Hz. Subjects wore a transparent infrared-blocking face shield (Selstrom 32130 with Shade 3 IR window, ∼.3kg) in order to allow the infrared cameras of the eye tracker to work in sunlight. The mask did not occlude subjects' field of view and affected vision similarly to green-tinted sunglasses. Kinematics were recorded using the Motion Shadow full body motion capture system using inertial measurement units recording at 100Hz ([56] provides a detailed technical description of a similar system). Raw data were initially recorded on a backpack-mounted MacBook Air worn by the subject (total weight, ∼2.5kg).

Kinematic data were down-sampled to match the recording rate of the eye tracker (30Hz). All post-processing analyses were performed offline using custom MATLAB code.

Experimental Task
Subjects walked across terrains of three different difficulties: Flat, Medium, and Rough. The paths used for each condition were selected to be relatively straight, relatively free from elevation gain, and to have a consistent level of difficulty along the entire path. All three paths were located near the Shoal Creek Greenbelt near the intersection of 29th St and Lamar Ave in Austin Texas ZIP 78705, USA. The Flat terrain (GPS (30.298769, −97.748752) – (30.298942, −97.747940)) condition was a packed earth trail containing very few obstacles, so little visual guidance was necessary to guide foot placement. The Medium terrain (GPS (30.298918, −97.748868) – (30.298840, −97.748905)) consisted of small (fist sized) to medium (head sized) rocks. Visual guidance was needed to place the feet, but finding an available foothold was relatively easy (most ground locations were viable footholds). The Rough Terrain (GPS (30.297891, −97.749898) – (30.297584, −97.750080)) consisted mostly of large boulders. Substantial visual guidance was necessary to support locomotion in this terrain, as the majority of viable footholds were located on the tops of boulders (that is, most ground locations were not viable footholds).

Experimental Protocol
Subjects began by putting on the equipment and taking a practice walk from the starting location to the end of the Flat terrain path. The experimenter followed the subject closely at all times. After the practice walk, subjects completed a calibration protocol described below. Following calibration, subjects completed a validation task whereby they walked across a flat path that contained 6 brightly colored markers on the ground arranged 3 m apart in a straight line. Subjects were instructed to traverse the path of markers while always maintaining fixation on the nearest marker. This data task was later used to validate the calibration procedure for each subject (See *Calibration Error and Validation*, below).

Subjects then completed 3 total trips to the end of the Flat Terrain path and back, for a total of 6 straight-line walks (~70.9 m per walk, ~420 m total). Subjects then moved to the Medium terrain path, completed a practice walk, repeated the calibration task, and then completed 3 total trips for 6 total straight line walks (~60 m per walk, ~360 m total). This procedure was repeated for the Rough terrain. The path used in the Rough terrain was slightly shorter than the other terrains, so subjects completed 4 total trips (8 straight line walks) in order to complete a comparable total distance (~40 m per walk, 320 m total). We did not note any substantial differences in behavior during repeated walking over the same terrain.

VOR-based calibration and data post-processing

The eye tracker recorded subject's point of regard (POR) in 2D pixel coordinates relative to the outward facing scene camera that was mounted on the subject's head. The kinematic data from the inertial motion capture system recorded movement in millimeters relative to magnetic north (determined by the triaxial magnetometers in the IMU sensors) and the gravity vectors (determined by the IMU accelerometers). In order to calculate subject's 3D gaze vector, it was necessary to situate the 2D data from the eye tracker into 3D reference frame of the motion capture system. To this end, we developed a calibration method that capitalized on the vestibular ocular reflex (VOR) to determine the proper alignment between the POR data from the eye tracker and the IMU coordinate system in order to recover subjects' 3D gaze vector relative to the body and world. Video S3 presents a video depiction of the optimization procedure to determine the orientation of the eye tracker's scene camera with the motion capture data. A reconstruction of a successful calibration procedure is shown in Video S4.

The calibration procedure was completed at the start of data recording for each terrain condition for later processing. Subjects stood on a calibration mat that had marks for the subjects' feet, a high visibility marker located 1 m ahead of the vertical projection of the midpoint of the ankle joint, and a 0.5 m piece of tape at the same distance. Following the experimenter's instruction, subjects maintained fixation on that point while slowly moving their heads up/down, left/right, and along the diagonals. In addition to help determine the subject's 3D gaze vector by relating eye and head movements, data from this portion of the record were used to calibrate the eye tracker (similar to the "head tick" method described in [59], except that our subjects moved their heads smoothly).

The post-processing procedure to calculate subject's 3D gaze was as follows:

1. **Scale pixel data into mm.** Identify the endpoints of the 0.5 m piece of tape in pixel coordinates. Use the ratio between the pixel distance and the true size of the tape to scale the data from the eye tracker into mm. This method assumes that the data from the eye tracker are situated on 2D plane located at the depth at which the eye tracker was calibrated (*calibrationDepth*)

2. **Synchronize the time stamps of the eye tracker and the motion capture system.** Because the eye tracker and the motion capture system were being recorded on the same backpack mounted laptop, the timestamps from the two systems were already synchronized. We verified this synchronization by examining the oscillations of the subjects' head and eye during the calibration procedure (Note that it would also be possible to synchronize the streams by identifying the temporal offset of the peaks in the eye and head oscillations).

3. **Downsample the 100Hz kinematic data to match the 30Hz data from the eye tracker.**

4. **Calculate the location of the camera within the reference frame of the subjects' head (*cameraXYZ*).** The location of the scene camera was calculated relative to the head marker data from the motion capture, and manual measurements of the eye tracking glasses. We identified this location on the first frame of the calibration procedure, and then generated its location for all subsequent frames by rotating this point in the head reference frame according to the orientation data from the head mounted IMU sensor.

5. **Place scaled POR data from the eye tracker onto a 2D plane whose normal vector intersects with the *cameraXYZ* point at a distance of *calibrationDepth*.** The 2D plane on which we place the POR data is equivalent to the far plane of the viewing frustum of the head mounted scene camera. At this point, the orientation of the camera on the subject's head is arbitrary. Identifying the correct orientation of the camera axis is the goal of the following steps.

6. **Project a line from the *cameraXYZ* point through each POR point on the viewing plane.** Each data point is now a 3D ray originating at the *cameraXYZ* point.

7. **Estimate the groundplane as an infinite 2D plane located 20mm below the subject's heel markers.**

8. **Identify correct orientation of the camera axis using unconstrained optimization (MATLAB's *fminunc* function, see Video S3).**
   a. Begin with a starting guess where the Euler angle rotation of the camera axis is [0 0 0].
   b. Rotate all gaze data by this rotation, and then rotate each gaze vector by the subject's head orientation on the frame that it was recorded.
   c. Calculate intersections between each gaze vector and the ground plane. If a gaze vector does not intersect the ground plane, truncate it at 10 m.
   d. Calculate error of this camera alignment rotation, defined as the mean distance between the intersection point of each gaze vector and the calibration point that subjects were fixating (located 1 m ahead of the vertical projection of the subject's ankle joints).
   e. Use fminunc to minimize this error by optimizing the Euler angle rotation to apply to the gaze vectors prior to applying the rotation specified by the subject's head orientation. The correct orientation will cause subjects' head rotations to cancel

their eye movements to maintain the gaze vector alignment with the calibration point (that is, the correct camera alignment rotation will preserve VOR-based eye compensation for head rotation).

9. **Once the correct camera alignment rotation has been identified, apply it to all subsequent gaze data from this recording prior to rotating each gaze point according to the subject's head orientation on that data frame. The end result of this calibration procedure may be seen in** Video S4**.**

Ground plane estimation

This calibration procedure generates a 3D gaze vector for each 2D POR data point from the eye tracker. Using these vectors, we determined subjects' ground fixations by calculating the intersection point between each gaze vector and the ground plane calculated for that frame. In order to correct for vertical drift in the IMU based kinematic data, the vertical position of the estimated ground plane was attached subjects' lowest heel marker on every frame. Frames in which the subjects' gaze vector did not intersect the ground plane within 5 leg lengths of the subject's location were discarded.

Reference frame definition

In each of the different terrains, subjects walked back and forth along the same path. For later analysis, each of these individual trips was cut out of the larger data recording and then translated and rotated so that each trip began with the vertical projection of the subjects' center of mass over the origin and ended on the +x axis. As a result, the global reference frame in this study defined the origin as the Start position of the walk, +x as the primary locomotor axis, +y as leftward, and +z as upward.

Sensor alignment correction

The IMU-based motion capture system derives its body segment orientation estimates by comparing the orientation of each sensor to a "root" sensor located over the subject's spine. Occasionally, a misalignment of this root sensor caused a horizontal offset in the head orientation relative to the body, which similarly offset the subject's gaze vector estimate. To correct for this misalignment, a single corrective rotation was applied to the subject's head orientation data in order so that the subject's gaze/ground intersections would be symmetrically distributed around their walking path. Importantly, this single angular offset was applied globally to an entire recording session, so it should not affect the relationship between gaze and gait behavior.

Calibration error and validation

During the calibration procedure described above, subjects fixated a point on the ground 1 m in front of them while moving their head in an up/down/left/right cross pattern. If the calibration procedure was perfect, subjects' gaze vectors during this procedure would all intersect with the calibration point with zero spread. In fact, the mean center of subjects' gaze vectors was 1.1 ± 0.45cm from the calibration point, with a standard deviation of 6.1 cm (See Videos S3 and S4). This distance corresponds to an error of about ± 1 degrees of visual angle, which is what would be predicted based on the combined error of eye tracker and head-mounted IMU.

To validate the calibration procedure, subjects walked along a straight path while fixating a series of small markers that were spaced 3 m apart along the path. If the calibration procedure worked properly, the resulting gaze/ground intersection should form clusters 3 m apart. The mean separation between the gaze/ground clusters was 2.83 ± 0.07 m. The slight underestimate of the distance between subsequent markers may stem from the upward bias in the drift of the IMU-motion capture suit (see below).

Known sources of measurement error

Some sources of error that are inherent in these research methods and equipment are listed below. Although this error does affect the data in this study, the analyses and arguments presented here were selected to be valid within the precision afforded by this methodology.

IMU drift

Position estimates based on IMU systems suffer from accumulating error, which causes drift on the order of about 1% of the length of the total movement [60]. The analyses in this study focus on data recorded within a distance of 2-4 steps relative to the body, so positional drift will be on the order of a few centimeters. Critically, sensor drift does *not* affect the frame-by-frame estimates of the orientation of the head relative to the body, which is essential for the ability calculate 3D gaze. The gaze estimates are only affected by sensor noise associated with the orientation estimates from head IMU (±1-2° during full-speed walking) and the noise from the eye tracker (±1°). The resulting estimated total error (±2-3°, ~10cm at a typical viewing distance) is in line with the results of the calibration procedures described above.

Parallax error

This marker used in the calibration procedure was located on the ground 1 m ahead of the subject, which resulted in an average calibration distance (eye to ground) of about 2 m (based on the mean subject height of 1.77 m). This distance was slightly less than the mean viewing distance (eye to ground) in this study. The mean look-ahead distance (distance along the ground plane between gaze location and the body) was 2.05 m for the Flat terrain and 1.35 for the medium and rough, corresponding to a viewing distance of about 2.3 m and 2.1 m, respectively. This mismatch between calibration and viewing distance imparted a small parallax error, where the error was < 1cm in the direction closer to the subject [59]. Even when subjects looked at further distances, parallax error remained small (2-3cm of error for look-ahead distance of 3-4 m, respectively).

Flat ground plane assumption

Because of the drift inherent to the IMU based motion capture system, the ground plane was estimated to be an infinite, flat plane attached to whichever heel marker was lowest on each recorded frame. This assumption allowed us to estimate gaze/ground intersection and mitigated many of the problems with drift in the position estimates from the IMU suit. However, assuming that the ground plane was flat led to error in our measures of gaze/ground intersection at least two ways: First, if the subject was looking at a raised rock that was in their path, our system would record that as an intersection with the groundplane behind that rock. For instance, if a 1.7 m subject was looking at a 0.2 m tall rock 1.5 m ahead of them, the system would report an intersection with the ground 1.7 m away. Similarly, if the was subject was standing on top of a rock looking a point lower than their planted foot, this would be reported as an intersection with ground closer than the subject was actually looking. Second, because the height of the ground plane was defined as the height of a subject's heel marker, this plane will move upward/downward as the subject stepped onto or off of a raised rock in their path. This would result in the location of the gaze/ground intersection drifting forward or backward even if the subject is actually fixating one location on the ground. It is difficult to estimate the effects of this source of error without a direct measurement of the geometry of the path. We expect that the effects will largely cancel out on average, although it will add to the variance. In any case, the analyses presented in this study should be robust to the type of error afforded by the flat ground plane assumption.

QUANTIFICATION AND STATISTICAL ANALYSIS

Summary of Statistical Analyses Used in This Study

Row	Measure	Comparison	t	df	p	Cohen's d	Mean Diff	95% CI Upper	95% CI Lower
1	Walking Speed	Flat versus Med & Rough	8.01	16	5.4e−7	4.01	0.44	0.56	0.33
2	Step Length	Flat versus Med & Rough	2.13	16	0.049	1.06	0.06	0.12	0.00
3	Step Duration	Flat versus Med & Rough	−2.26	16	0.038	−1.13	−0.04	0.00	−0.09
4	Step Length Duration Half Max	Flat versus Med & Rough	−3.15	16	0.006	−1.58	−0.04	−0.01	−0.07
5	Proportion of Gaze on Ground	Flat versus Med & Rough	−5.56	16	4.3e−5	−2.78	−0.37	−0.23	−0.51
6	Proportion of Gaze on Ground	Flat versus Med	−3.75	10	0.004	−2.17	−0.36	−0.15	−0.58
7	Proportion of Gaze on Ground	Flat versus Rough	−3.93	10	0.003	−2.27	−0.38	−0.16	−0.60
8	Proportion of Gaze on Ground	Med versus Rough	−1.08	10	0.306	−0.62	−0.02	0.02	−0.05
9	Delta Max Probability	Flat N+2 versus N+1,3,4	1.88	22	0.073	0.89	0.13	0.27	−0.01
10	Delta Max Probability	Med N+2 versus N+1,3,4	2.22	22	0.037	1.04	0.42	0.81	0.03
11	Delta Max Probability	Rough N+2 versus N+1,3,4	5.09	22	4.2e−5	2.40	0.94	1.33	0.56
12	Sum Density Near Origin (Full Step)	Med N+2 versus Med N+ 3	3.16	10	0.010	1.83	0.17	0.28	0.05
13	Sum Density Near Origin (Full Step)	Rough N+2 versus Rough N+3	0.76	10	0.465	0.44	0.03	0.12	−0.06
14	Path Straightness	Flat & Med versus Rough	12.12	16	1.7e−9	6.06	0.26	0.30	0.21
15	Path Straightness	Flat versus Med	1.67	10	0.126	0.96	0.04	0.10	−0.01
16	Path Straightness	Flat versus Rough	16.71	10	1.2e−8	9.65	0.28	0.31	0.24
17	Path Straightness	Med versus Rough	10.41	10	1.1e−6	6.01	0.23	0.28	0.18
18	Sum Density Near Origin (Early Step)	Med N+2 versus Med N+ 3	5.07	10	4.8e−4	2.93	0.24	0.35	0.14
19	Sum Density Near Origin (Early Step)	Rough N+2 versus Rough N+3	3.22	10	0.009	1.86	0.11	0.18	0.03
20	Sum Density Near Origin (Late Step)	Med N+2 versus Med N+ 3	2.63	10	0.025	1.52	0.17	0.31	0.03
21	Sum Density Near Origin (Late Step)	Rough N+2 versus Rough N+3	−0.66	10	0.525	−0.38	−0.03	0.08	−0.15
22	Look-Ahead Distance	Flat versus Med & Rough	3.88	10	0.003	2.18	0.84	1.36	0.37
23	Look-Ahead Distance	Flat versus Med	3.88	10	0.003	2.24	0.87	1.36	0.37
24	Look-Ahead Distance	Flat versus Rough	3.36	10	0.007	1.94	0.82	1.36	0.28
25	Look-Ahead Distance	Med versus Rough	−0.32	10	0.757	−0.18	−0.05	0.30	−0.40
26	Look-Ahead Time	Flat versus Med & Rough	0.74	10	0.474	0.13	0.04	0.53	−0.27
27	Look-Ahead Time	Flat versus Med	0.74	10	0.474	0.43	0.13	0.53	−0.27
28	Look-Ahead Time	Flat versus Rough	−0.25	10	0.808	−0.14	−0.05	0.40	−0.50
29	Look-Ahead Time	Med versus Rough	−1.53	10	0.156	−0.89	−0.18	0.08	−0.45

Each row shows the results of a within-subjects paired *t* tests.

In order to determine the relationship between gaze and upcoming footholds, we began by situating subjects' gaze on the ground in a reference frame centered on their planted foot. We began by splitting up each straight-line walk into individual steps, where each step was determined as the period between heelstrike of a given foot and the frame before the heelstrike of the other foot (that is, each step period began at the onset the double support phase and continued until the end of single support, or one frame prior to the onset of the subsequent double support). For each recorded gaze intersection with the ground, we subtracted the (x,y) ground plane coordinates of the gaze intersection with the (x,y) ground plane coordinates of the heel marker of the stepping foot. This method had the effect of centering subjects' gaze on the location of their planted foot.

In addition to calculating gaze relative to the location of the subjects' planted foot (Foothold N), we also represented it relative to the location of the steps that were upcoming (Foothold N+1 – 4) at the time that the gaze vectors were recorded. The procedure for this process was identical to the method used to align gaze to the planted foot, only now instead of subtracting the (x,y) location of the planted foot from each gaze point, we subtracted the (x,y) locations of the foothold location of the steps that were coming up in the future. In all we represented subjects' gaze in 5 different reference frames – one centered on the planted foot (Foothold N), one centered on the first upcoming step (Foothold N+1, i.e., the destination of the currently swinging foot), and one each for Foothold N+2, N+3, and N+4.

Calculating gaze density

Gaze density in each of the step-centered reference frames was calculated using a Gaussian kernel density estimate. Each recorded data point was replaced with a 2D Gaussian with a sigma of 0.05 leg lengths and a sum of 1. These Gaussians were summed (at a 2D bin size of 0.01 leglengths^2) and then normalized by the total duration of each straight-line walk to determine the probability distribution of subjects' gaze in each of the reference frames. Note that the probability was normalized by the total number of recorded frames in each walk, which was larger than the number of gaze intersections with the ground plane (because not all of the subjects' gaze vectors intersected the ground plane). As a result, the sum of the total probability distribution in each reference frame was equal to the proportion of the time that subjects spent looking at the ground.

Subsequent analyses of each subjects' gaze density distribution for each reference frame were as follows:

1. **ΔMax Probability (Figure 4A)** – For each condition, the peak probability for each reference frame was identified and divided by the peak probability of the planted foot (Foothold N) reference frame. This analysis showed the proportional increase in the peak of the probability distribution of gaze in each reference frame relative to the peak probability of the planted foot reference frame.

2. **Gaze Variability (Figure S2)** – The variability of each of the step-centered probability distribution was estimated as the sum of the bins of the gaze density distribution that had a value equal to or greater than half of the maximum probability of that distribution.

3. **Gaze Density Near Origin (Figure 4B)** – The ΔMax Probability and Gaze Variability analyses both examine the entire probability distribution for each gaze density distribution in order to provide insight into the relationship between gaze and upcoming footholds. However, these results may be misleading when considering the way that subjects plan individual footholds, as the strong correlation between subsequent steps may affect the gaze distribution in each foothold-centered reference frame. For instance, if we imagine that subjects *always* fixated on the location of Foothold N+2, this would result in an increase in the probability distribution in the Foothold N+1 reference frame due to the strong correlation between the location of Foothold N+1 and the location of Foothold N+2 (e.g., note that in Figure 3, the peak of the probability distribution in the Foothold N+1 reference frame in the Medium terrain is roughly one step length ahead of the origin). To correct for this correlation, we also calculated the sum of the probability of the bins of the gaze probability distribution that were within 0.3 leg lengths of the origin in each step-centered reference frame. This analysis shows the proportion of the time that subjects spent looking at that upcoming step (which is defined as the origin in each of the step-centered reference frames).

In addition to the gaze probability based analyses, we also calculated 1D histograms showing the subjects spatial and temporal look ahead in each of the terrain conditions. To determine spatial look ahead, we calculated the Euclidean distance between the position of the subjects' center of mass and gaze point on every recorded frame, discarding frames where gaze was more than 0.5 leg lengths of walking path (i.e., greater than 0.5 leg lengths from any future COM location). To calculate temporal look ahead, on each frame we determined the amount of time that would elapse between the current frame and the time that the subject would pass the point on the path that they were currently looking at (i.e., how long until they reached the COM position nearest to the point on the ground they were looking at).

Statistics

Paired t tests were used to compare within-subjects means for relevant analyses. Statistical analyses are summarized in table in Quantification and Statistical Analysis.

DATA AND SOFTWARE AVAILABILITY

The raw and post-processed data utilized in this study is available via Figshare, along with the MATLAB code necessary to access and analyze it: https://doi.org/10.6084/m9.figshare.6130850.